

Impacts of In-stream Sand mining on the River Geometry in Aleto Eleme, Rivers State Nigeria

Jeremiah Uriah Richard¹, ² Jonah Iyowuna, Benjamin²
Godwill Tamunobiekiri Pepple³

¹Head Survey Coordination, Office of the Surveyor General, Moscow Road, Port Harcourt, Nigeria,

²Surveying and Geo informatics, Rivers State University, Nkpolu – Oroworokwu, Port Harcourt, Nigeria,

³Surveying and Geo informatics, Rivers State University, Nkpolu – Oroworokwu, Port Harcourt, Nigeria,

Date of Submission: 05-09-2025

Date of Acceptance: 15-09-2025

ABSTRACT

Sand is a free gift of nature. It is available in wetlands, rivers, creeks, streams and dry land. Its demand is constantly on the increase and the search for sand also increased. They are used for the construction of roads, buildings, bridges, land reclamation etc. In-stream sand mining modifies the natural geometry of the river. The modifications may be on both length and width which can be studied using remote sensing and GIS techniques. In this study, NDWI was utilized to study changes in river geometry due to sand mining in Aleto Eleme River. The study was carried out using six epochs (2000, 2005, 2013, 2015, 2018 and 2021) of Landsat imageries. The selected Landsat image was the L1 which has been corrected for geometric distortions. Landsat data was converted from grey value to radiance image using the algorithms specified in the Landsat metadata. Green and near infrared bands of each epoch were used to compute NDWI. The results of the analysis revealed that NDWI of water bodies are 0.20 – 0.35, 0.20 – 0.32, 0.24 – 0.41, 0.22 – 0.35, 0.22 – 0.37 and 0.27 – 0.36 for the years 2000, 2005, 2013, 2015, 2018 and 2021 respectively. It is water if $NDWI > 0.20$ and non-water if $NDWI < 0.20$. Also, there is a general increase in water body due to sand mining. In 2000 the width of the river was 122m in the west but increased to 146m in the year 2013. The width increased to 152m in the west and 309m in the east in 2015. Also, it increases in width to 360m in the west and 515m eastward in 2021. The length of the river also increased from 1071m in 2000 to 3337m in 2021. NDWI is an effective remote sensing and GIS tool in mapping changes in water geometry. Further study should compare manual extraction of river boundary using

high spatial resolution satellite image with the results of NDWI.

Keywords: Aleto Eleme, Landsat Image, NDWI, Sand Mining, River Geometry, Remote Sensing

I. INTRODUCTION

Sand like other commodities is highly demanded across the globe. Sand is the second most valuable resource after water [1] and the most commonly mined resource [2]. Globally, 85 per cent of mining activities is sand with a total volume extracted per year value over 40 billion tonnes [2] with 30 per cent of it used for construction purposes [1]. In England and Wales about 20 - 25 million tonnes of sand are mined each year with over 20 per cent of the sand used for construction purposes [3]. It is naturally available for human utilization. Sand as seen by many professionals is defined differently. The geologists defined sand as grain with upper size boundary of 2mm and the lower size as 0.0625mm. Sand is also defined by the Unified Soil Classification System as material with grain size between 0.075mm and 4.75mm [4]. It is formed by erosive action of rivers, streams, and lakes [5]. Sand is an aggregate consisting of sand of various grain sizes, pebbles, and gravel. It is being used on a daily basis as raw materials for the production of specific products. It is used in the production of concrete, glass, and road construction [6], [2]. Sand is used for the extraction of oil and gas from rocks by a system called fracking [7]. Frack sand is in high demand in those countries that utilized the technology in the oil and gas industries. Industrially, sand is used in the production of Zircon ($ZrSiO_4$) which is an additive to metal alloys, chemicals and foods. Also, sand is used by nuclear and aerospace industries for

the production of titanium [2]. Most importantly, sand is used for land reclamation works, road embankment, and shoreline protection [5].

Besides social and economic importance of sand, there are still health and environmental risks associated with sand mining. Sand mining causes respiratory disease, damage farmland [8] and climate change [9]. Sand mining resulted in the alteration of river, estuaries and stream topography and loss of biodiversities [10]. Sand mining in Hallsands on the Devon Coast directly impacted on their home with many homes destroyed [11]. This is similar to what is happening in an areas subjected to excessive dredging. In those areas farm land, access roads, bridges and natural beach are lost due to sand mining. In addition, aquatic organisms are being severely affected during sand mining by dredging. Sand dredging has direct and indirect impacts on aquatic organisms [12]. Some aquatic organisms may be in extinction due to the pollution of estuary.

The global demand for sand defers with some countries having abundance sand deposit to export and other countries depends on imported sand for their urban development. Based on the world trade statistics on sand, Singapore is the world largest importer of sand while United States of America remains the largest exporter of sand [13]. In the trade reports, Singapore imported sand valued 366USD and United States exported 531USD of sand in 2018 alone. Global demand for sand will be skyrocket in the coming years as cities and estates are being developed to march urban population.

Shorelines are the most impacted land area during sand mining. It is always in direct contact with the mining areas and as such suffers severe degradation and change. The degradation of the shoreline may be caused by the dredging machine or caused during the clearing for stockpiling. It may also be caused by transportation of sand from the site to a destination. [14] reviewed the impact of sand mining on the coast of Morocco, Kerala in India, Kwale in Kenya, and Santa Barbara Beach in Azores. According to him, sand mining has led to change in the channel geometry. [15] observed that the shoreline erosion is at increase in a sand mining environment. [16] stated that these changes in

shoreline geometry can be studied using aerial photographs of different epochs. [17] used satellite images, maps, and meteorological wind statistics to study shoreline change due to sand mining in Turkey Black Sea coast. The study examines the geometry of a pit on the shore over a period of years. [18] used Digital Shoreline Analysis System (DSAS) software to study coastline change due to sand mining and observed rate of change for seven years (2005-2012) as 0.85m/year. This study was aimed at mapping change in river geometry from 2000 to 2021 using Normalized Difference Water Index (NDWI) which is capable of differentiating water from non-water on satellite imageries.

1.1 Study Area

The study area is Aleto River in Eleme Local Government Area Rivers State, Nigeria. It is located on 531000mN - 532200mN and 286000mE – 291200mE in the Zone 32N. The river is a tributary of Elenwo River and is tidal in nature. The length of the section of the river under study is 3,700m with a natural width of 25m – 38m. It is approximately 1,600m to the left and 2,100m to the right of Aleto Bridge. It is also about 1000m from the Eleme Petrochemical Company. The section of the river used for the study is crossed with a bridge by the popular East/ West Road (dual carriage way) owned and maintained by the federal government of Nigeria. Sand mining is being carried out on both sides of the bridge at close distance. Hydraulic dredging is being used to mine sand in the area. Sand mining in the area started around 2000 on a relatively small holding and now the activities of sand mining cannot be control. It has spread to kilometers along the shore. The entire stretch of the river has been degraded as a result of sand mining. The degradation was not only on the river channels but also on the transportation routes used by tippers to transport sand. The access roads (untarred) leading to the sand dumps has become so deep that the difference in height between the natural surface and the degraded roads is about 1.5m high.

Land use/ cover in the area are wetland covering the bank of the river and spread up to 300m wide, built-up locating as close as 160m to the river, access roads mostly untarred, and farm land.

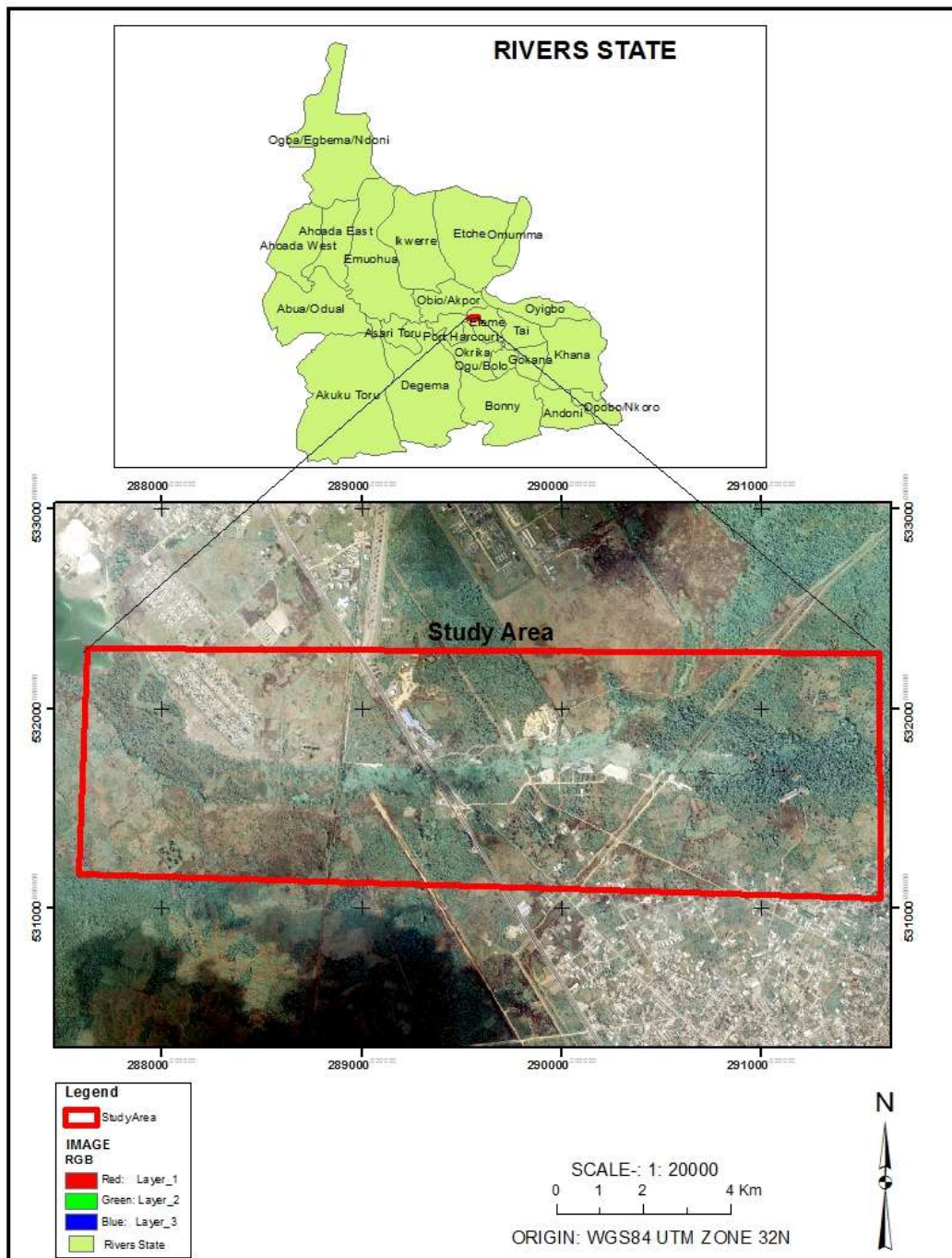


Figure 1.1 Study area map produced from SPOT image and shapefile of Rivers State.

II. METHODOLOGY

The study was aimed at determining changes in river geometry for six epochs (2000 to 2021). Landsat satellite imageries were used to derive NDWI after converting raw images to TOA.

NDWI for each epoch were used to compute change in river geometry caused by sand mining in Aletto River. Figure 2.1 shows flow chart methodology for the study.

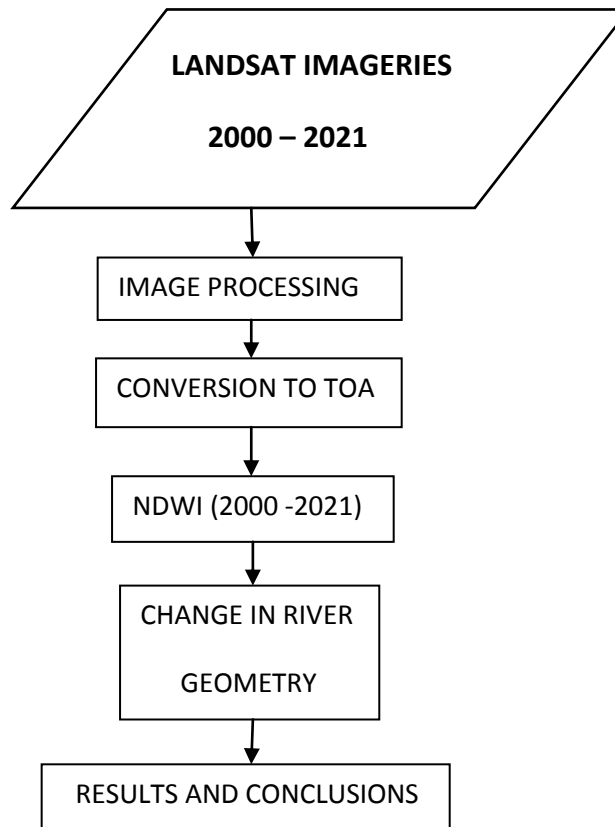


Figure 2.1 Research flow chart.

2.1. Dataset and Software

The study used remote sensing data and GIS software to mapped change in river geometry. ESRI’s ArcGIS 10.3.1 was selected for the study because it has the ability to performed raster calculations. It was used to perform image clipping, computation of NDWI and compilation of maps. ArcGIS strength was in vector analysis.

Landsat data was the main dataset used for the mapping of change in river geometry associated with sand mining. Landsat image selection was based on it availability to all researchers and can be

feely downloaded. Changes in river geometry were obtained from Landsat imageries of six epochs (2000 – 2021). In 1972, the first Landsat mission was launched into space [19]; [20]. The mission was aimed at mapping and monitoring the earth surface. Presently, Landsat mission has improve from 8 to 11 bands with the additional capability in discriminating earth’s surface features. The data was downloaded from its website <http://glovis.usgs.gov/> free-of-charge. The characteristics of the Landsat satellite imageries utilized for the study are shown in table 2.1.

Table 2.1 Characteristics of Landsat imageries used for the study.

Sensor	Path/ Row	Imagery Date	Resolution (m)	Bands
Landsat ETM (L7)	188/ 57	17/12/2000	30 x 30	B2 and B4
Landsat ETM (L7)	188/ 57	13/01/2005	30 x 30	B2 and B4
Landsat ETM (L7)	188/ 57	03/01/2013	30 x 30	B2 and B4
Landsat ETM (L7)	188/ 57	22/12/2015	30 x 30	B2 and B4
Landsat OLI (L8)	188/ 57	27/12/2018	30 x 30	B3 and B5
Landsat OLI (L8)	188/ 57	18/02/2021	30 x 30	B3 and B5

2.2 Image Processing

Landsat image has been corrected for geometric and radiometric distortions by the data provider and as such no need for corrections. The data has been correctly referenced to World

Geodetic System 84 (WGS84) [20]. Landsat imageries used for the study were obtained from different epochs (2000 – 2021). Some of these data contained periodic line dropout which required correction before usage. The epochs that contained

periodic line dropout are Landsat 2005, 2013 and 2015. Periodic line dropout appears like gap on the remotely sensed image [21]. The gaps were caused by failure of the sensor Scan Line Collector [22]. In PANCROMA™ five gap filling methods are available but Hayes interpolation method was used because of its computational approach in gaps filling [21]. PANCROMA™ corrected for gaps in the image by using two images, one with gaps and another without gaps. Landsat 2005, 2013 and 2015 were corrected for periodic line dropout using another image of same year and without gap for their corrections.

Accordingly, Landsat imageries were converted from Digital Numbers (DNs) to radiance image. [23] also converted Landsat data from DNs to radiance before application in surface water mapping. Radiance image represents earth surface physical units used for calculations [20]. The algorithm for the conversion is different depending on the sensor used. For L8, the radiance algorithm is giving by

$$L_{\lambda} = M_L \times Q_{cal} + A_L \text{ ----- } 1$$

Where, L_{λ} is the spectral radiance in $Wm^{-2}Sr^{-1}$, M_L is the radiance multiplicative scaling factor for the band, Q_{cal} is the L1 pixel value in DN and A_L is the radiance additive scaling factor for the band [20]. Similarly, the algorithm for the conversion of L5 and 7 to radiance image is giving by

$$L_{\lambda} = (LMAX_{\lambda} - LMIN_{\lambda}) / (QCALMAX - QCALMIN) \times (DN - QCALMIN) + LMIN_{\lambda} \text{ ----- } 2$$

Where, $LMAX_{\lambda}$ is the maximum spectral radiance for the band, $LMIN_{\lambda}$ is the minimum spectral radiance for the band, $QCALMAX$ is the maximum quantize calculated for the band, $QCALMIN$ is the minimum quantize calculated for the band and DN is pixel DN value [20].

The conversion was performed in ArcGIS ArcToolbox using raster calculator by substituting the bands values specified in the Landsat metadata file. The radiance images were used to compute NDWI used in analyzing impacts of sand mining from 2000 to 2021.

2.3 Normalized Difference Water Index (NDWI)

The impacts of sand mining activities on the river geometry were determined using NDWI. NDWI is a remote sensing tool that is very useful

in discriminating water body from non-water body. [23] used NDWI to carry out change detection on surface water in Nepal. [24] also used NDWI to extract surface water bodies in Vietnam. Also used in mapping flood water [25]; [26]. NDWI algorithm was first proposed by McFeeters in 1996 and is giving by

$$NDWI = (Green - NIR) / (Green + NIR) \text{ ----- } 3$$

In this work, McFeeters set zero (0) as the threshold for water and non-water. The values range from -1 to 1 with value above zero are water body and less or equal zero as non-water [27], [28]. Like NDVI, NDWI is a dimensionless index since it is giving by the ratio of two radiance images. NDWI can be derived from medium and low spatial resolution satellite images. [29] have used Moderate Resolution Imaging Spectroradiometer (MODIS) to derive NDWI and [30]; [25] used Sentinel-2 to derive NDWI in Mediterranean region and River Buna. In this study, Landsat data was used to derive NDWI. From the NDWI algorithm for L5 and 7, green is band 2 and near infrared is band 4 but for the L8, green is band 3 and near infrared is band 5. The bands used were the radiance converted in ArcGIS 10.3.1. NDWI showing the impacts of sand mining on river geometry was computed for 2000, 2005, 2013, 2015, 2018 and 2021.

III. RESULTS AND DISCUSSIONS

The results show the changes in river geometry from 2000 to 2021 as obtained from NDWI analysis. NDWI maps were classified into three classes and each class represents particular land cover. The results of the 2000 NDWI map was shown in figure 3.1a. For the 2000 NDWI map, values range from -0.09 to 0.35. The first class ranges from -0.09 to 0.06 and are located more in the east and north of the map. The second class ranges from 0.06 to 0.20, representing built-up and roads. The last class was water body and ranges from 0.20 to 0.35. Water body was seen in two isolated locations to the left of the map as represented with Moorea blue. Figure 3.1b was the 2005 NDWI map with values range from -0.01 to 0.32. Water body ranges from 0.20 to 0.32 and built-up ranges from 0.10 to 0.20. The vegetation has NDWI of -0.10 to 0.10, covering the larger area of the map.

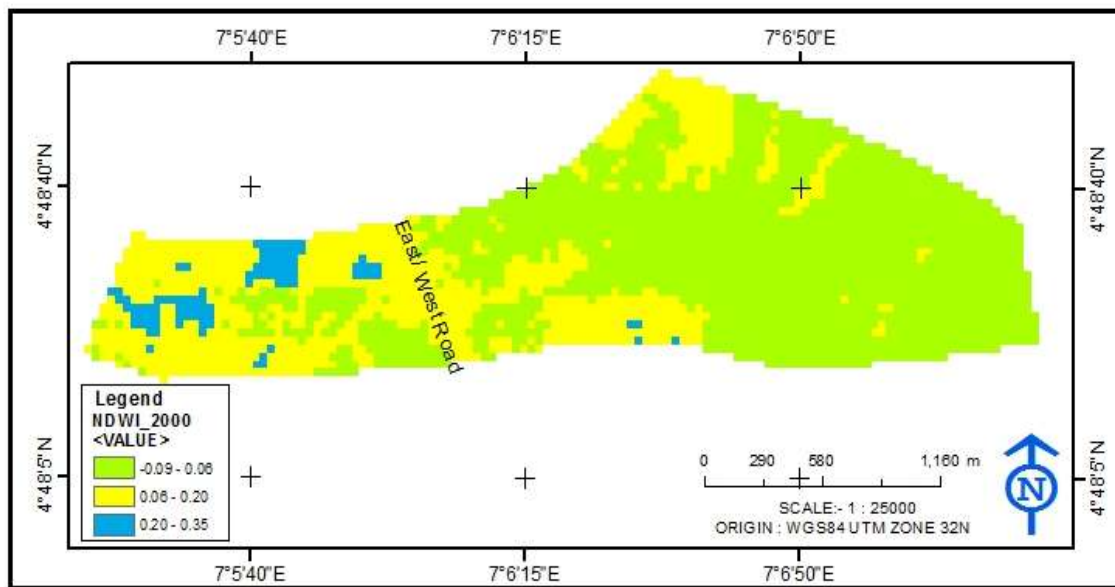


Figure 3.1a NDWI map of 2000.

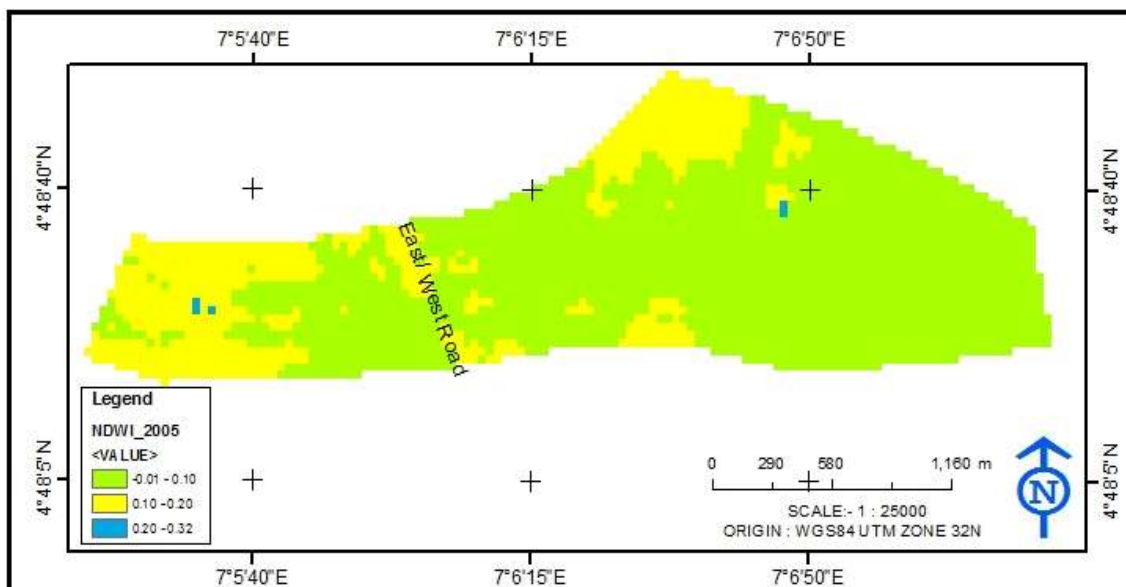


Figure 3.1b NDWI map of 2005.

In 2013 NDWI map the impact of sand mining on the river geometry is as shown in figure 3.1c. The minimum and maximum values of NDWI are -0.09 and 0.41. High value indicates water body while lower value indicates vegetation. Within classes, water body ranges from 0.24 to 0.41 while built-up ranges from 0.08 to 0.24. Vegetation ranges from -0.09 to 0.08 as shown in green.

Similarly, figure 3.1d was the NDWI map of 2015 with the minimum value -0.05 and maximum value 0.35. The first class was the vegetation with NDWI value ranges from -0.05 to 0.09 while the last class was the water body with value ranges from 0.22 to 0.35. Water body increased in size and extended towards the east.

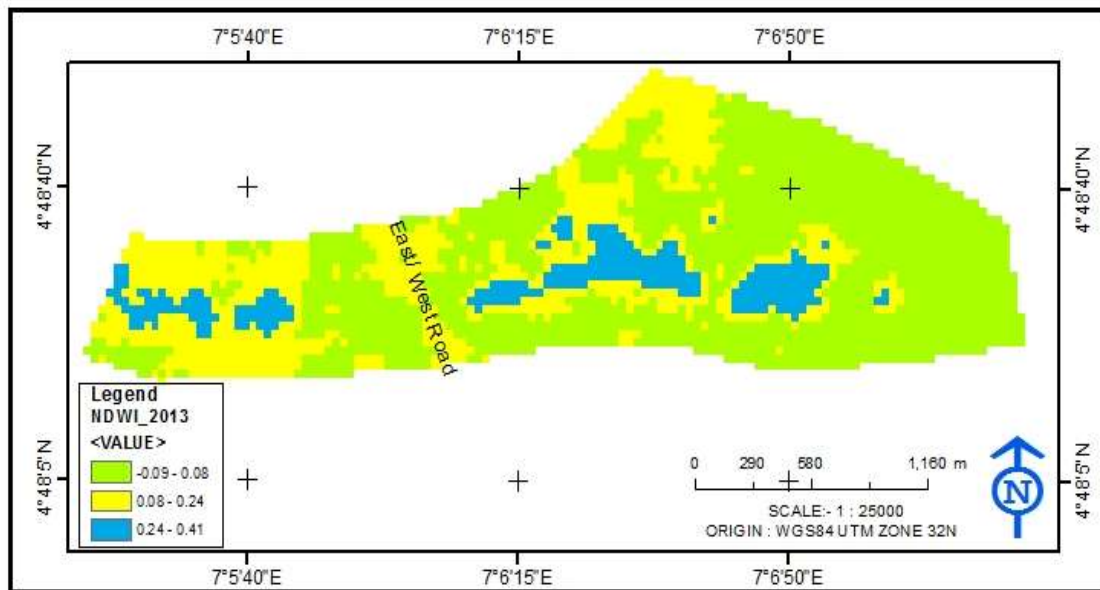


Figure 3.1c NDWI map of 2013.

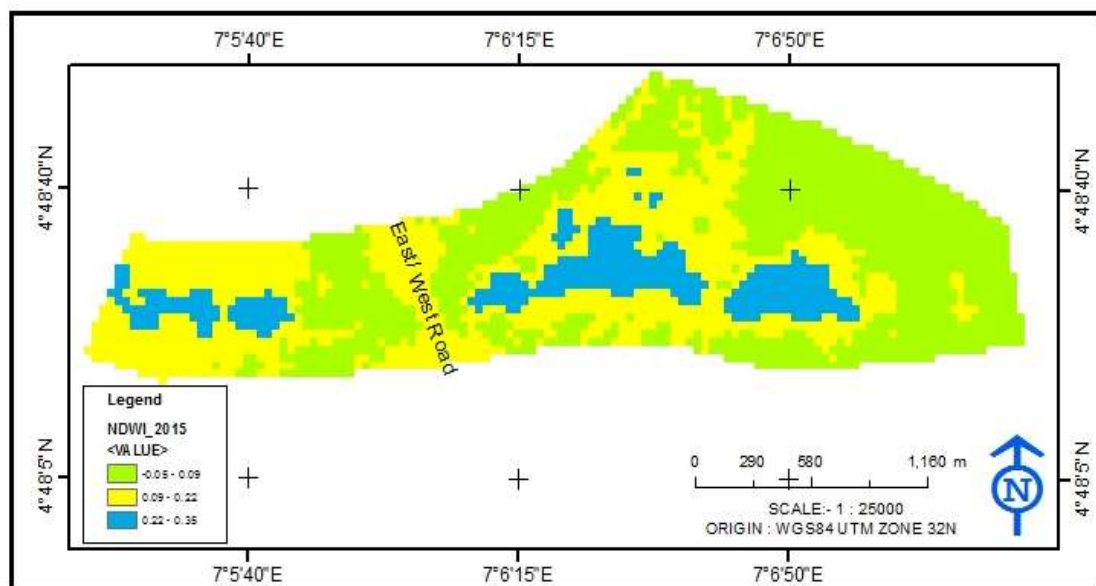


Figure 3.1d NDWI map of 2015.

Also, figure 3.1e was the 2018 NDWI map. The minimum and maximum NDWI values are -0.08 and 0.37. The first class was the vegetation and the NDWI values ranges from -0.08 to 0.07 and the second class was the built-up with values ranges from 0.07 to 0.22. The last class is the water body with values ranges from 0.22 to

0.37. Similarly, in 2021 NDWI map as shown in figure 3.1f, the minimum and maximum values are 0.08 and 0.36. The section representing water body lied within the range of 0.27 and 0.36. NDWI value of vegetation ranges from 0.08 to 0.17 and built-up was 0.17 to 0.27. The size of water body increase northwards.

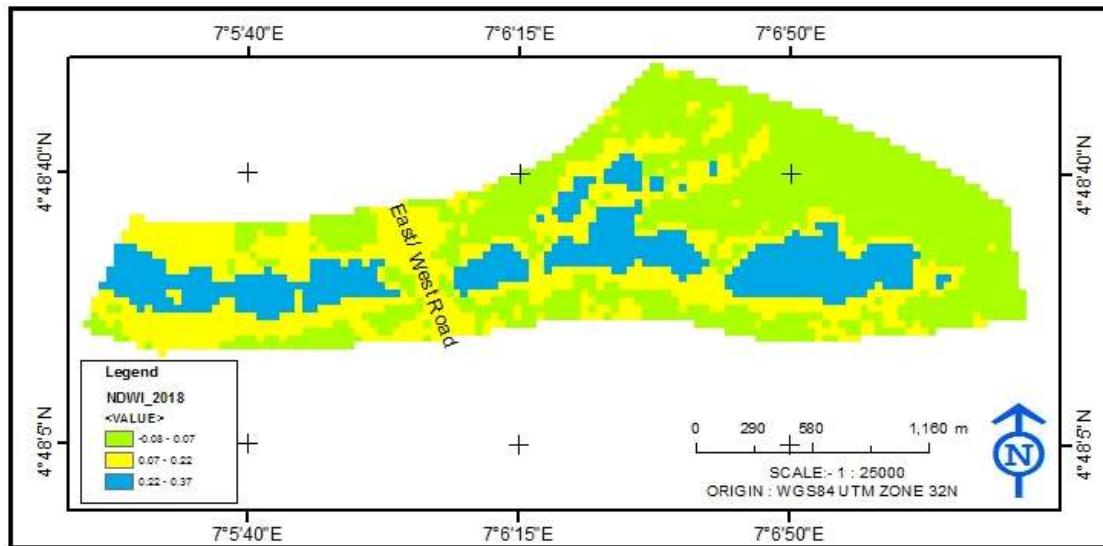


Figure 3.1e NDWI map of 2018.

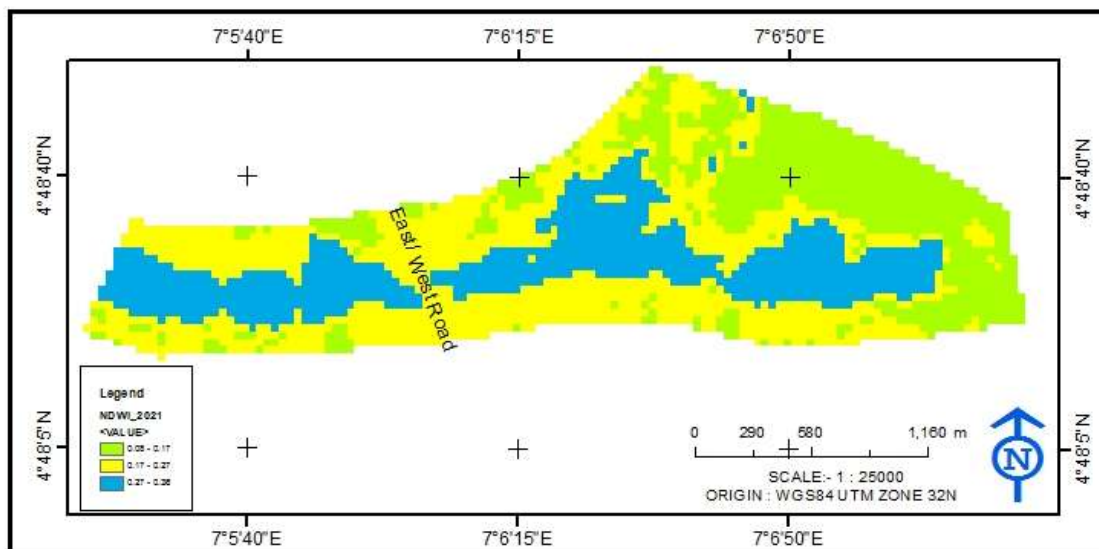


Figure 3.1f NDWI map of 2021.

Discussions

In 2000, sand mining activities were limited to small section in the west which modified river geometry from the narrow strip to width of 122m. In 2005 the water body reduces in areal extent probably due to a reduction in sand mining. Sand mining locations might have regrowth and cover the water surface which gave rise to small water body in 2005. Secondly, it is believed that the width of the river may be less than the resolution of the image in 2005. In 2013, river geometry increased in width and length, indicating resumption of sand mining. The increase was towards the east and across the Aletto Bridge. The width in the west increased to 146m and in the east

in one of the section along the river it increased to 211m with large irregular shape. River width has increased in the west by 24m between 2000 and 2013. In 2015, the width of the river increased to 152m in the west and increased in width to 309m eastward. There was an increased in width of the river in the west by 6m and in the east by 98m between 2013 and 2015. This large difference indicates increase in sand mining in the east. In 2018, there was an increase in the width and length of the river as a result of sand mining. This increase occurred from west (before the bridge) and toward east (across the bridge). The width of the river channel increase to 220m in the west and 481m in the east. In 2021, the width increase in one section

to 251m and in another section to 360m in the west. Similarly, in the east, the width increased to 515m and encroached landward. Net River Movement (NRM) at these two locations (west and east) using 2000 as baseline was calculated. NRM was calculated using 2013 as the oldest and 2021 as the youngest river boundary [31]. In the west NRM was 214m and 304m in the east. Sand mining has converted wetland, bare land and vegetation into water bodies. In addition, valuable land for urban development has been gradually cleared for sand mining. The impacts were occurring on both sides of the river. The size of the water bodies on the NDWI map increases but the NDWI values varies from one map to another. In general, the value of NDWI for water body for the six epochs ranges from minimum 0.20 to maximum 0.41. The highest NDWI value was in 2013 with value 0.41. Therefore it is water body if within this range. The NDWI results conformed to the manually extracted river boundary except for those years with the width of water body less than resolution of the image.

IV. CONCLUSION

River geometry is dynamic in nature and responded to both natural and human induce activities. Like shorelines, river geometry can be modified by sand mining. The modification can occur in both the length and width. Changes in river geometry can be obtained by digitizing river boundary or by image classification. The utilization of NDWI for mapping changes in river geometry due to sand mining has not been fully explored. This study sought the utilization of NDWI derived from Landsat imageries of six epochs to map change in river geometry in Aletu Eleme, Rivers State, Nigeria. Landsat datasets were converted from DNs to radiance image using the algorithms for L5 and L8 specified in Landsat metadata file. The radiance image was used for the computation of NDWI and the changes in river geometry were determined. The results of the analysis revealed that water bodies have NDWI value ranges from 0.20 to 0.41. Which means it is water body if > 0.20 and non-water if < 0.20 . The results also showed that river geometry has change from narrow channel to as wide as 515m in 2021. The change in river geometry was as a result of sand mining which modifies the width and length of the river. Further study should applied high spatial resolution like Sentinel-2 for an improvement in delineation of river boundary. Also, direct extractions of river geometry with high spatial resolutions imageries should be compare with

NDWI results which will better improve research outcome.

Conflict of Interest

This article emanated from the authors and they have declared that no conflict of interest with any person or organization.

REFERENCES

- [1]. World Bank Group (2018). What can be done about West Africa's Disappearing Sand? Knowledge Sheet 78, www.worldbank.org/waca, pp. 1-4.
- [2]. Mahadevan, P. (2019). Sand Mafias in India - Disorganizing Crime in a Growing Economy, Global Initiative against Transnational Organized Crime, www.GlobalInitiative.net, pp. 1-27.
- [3]. The Crown Estate (2013). Marine Aggregate Dredging and the Coastline: a Guidance Note, 16 New Burlington Place London W1S 2HX, www.thecrownestate.co.uk, pp. 1-27.
- [4]. Africa Community Access Programme, (2013). Guideline on the use of Sand in Construction in the SADC Region AFCAP/GEN/028/C, InfraAfrica (Pty) Ltd, Botswana CSIR, South Africa TRL, Ltd, UK Roughton International, UK CPP Botswana (Pty) Ltd, pp. 1-90.
- [5]. UNEP Global Environmental Alert Service (GEAS), (2014). Sand, Rarer than one Thinks, pp. 1-15.
- [6]. Aurora, T., Jianguo J. L., Jodi, B., and Kristen L. (2017). The World is facing a Global Sand Crisis, Boise State University Scholar Work, pp. 1-6.
- [7]. Thomas, M. P., and Donovan, S. P. (2013). The Economic Benefits of Costs of Frack – Sand Mining in West Central Wisconsin, pp. 1- 55.
- [8]. International Institute for Sustainable Development, (2018). Global Trends in Artisanal and Small – Scale Mining (ASM): A Review of Key Numbers and Issues, Intergovernmental Forum on Mining, Minerals, Metals and Sustainable Development, 1100-220 Laurier Ave, W. Ottawa, Ontario Canada R3B OT4, pp. 1- 91.
- [9]. Central Degrading Association, (2012). Climate Change Adaptation as it Affects the Dredging Community, Radex Building Rotterdamseweg 183C 2629 HD Delft, the Netherlands, www.dredging.org, pp. 1-6.

- [10]. ICES Cooperative Research Report, (2001). Effects of Extraction Marine Sediments on the Marine Ecosystem, In the Working Group on the Effects of Extraction of Marine Sediments on the Marine Ecosystem (Ed.), Palaegade 2-4 DK-1261 Copenhagen K Demark, pp. 17, 18.
- [11]. Vincent, M. (2007). Impacts on Beach and Cliff Stability Associated with Extraction of Sediments from Beaches and Offshore: Understanding the Communities Responses to Perceived Risk, Proceedings of Coastal Zone 07 Portland, Oregon July 22 to 26, 2007, pp. 1-5.
- [12]. Todd, V. L. G., Ian, B. T., Jane, C. G., Erica, C. N. M., Nicola, A. M., Nancy, A. D., and Frank, T. (2015). A Review of Impacts of Marine Dredging Activities on Marine Mammals, ICES Journal of Marine Science, Vol. 72, No. 2, pp. 328-340. doi:10.1093/icesjms/fsu187
- [13]. Lauren, K. (2019). Wave of Global Trade May be Depleting Beaches, International Trade, <https://www.globaltrademag.com/wave-of-global-sand-trade-may-be-depleting-beaches/>
- [14]. Pitchaiah, P. S. (2017). Impacts of Sand Mining on the Environment – A Review, SSRG International Journal of Geo Informatics and Geological Science (SSRG-IJGGS), Vol. 4, No. 1, pp. 1-5.
- [15]. GESAMP (2019). Sand and Gravel Mining in the Marine Environment – New insights on a growing environment problems submitted by the co-leads of the Correspondence Group, 46th Session Agenda item 7, pp. 1-37.
- [16]. Department of Irrigation and Drainage (2009). Sand Mining Management Guideline, Ministry of Natural Resources and Environment Department of Irrigation and Drainage Malaysia, Jalan Sultan Salahuddin 50626 Kuala Lumpur, Malaysia, ISBN 978-983-41867-2-2, pp. 16.
- [17]. Demir, H., Otay, E. N., Work, P. A. and Borekci, O. S. (2004). Impacts of Dredging on Shoreline Change, Journal of Waterway Port Coastal and Ocean Engineering, Vol. 130, pp. 170-178. 10.1061/~ASCE!0733-950X~2004!130:4~170!
- [18]. Jonah, F. E., Adjei-Boateng, D., Agbo, N. W., Mensah, E. A. and Edziyie, R. E. (2014). Assessment of Sand and Stone Mining along the Coastline of Cape Coast, Ghana, Annals of GIS, Vol. 21, No. 3, pp. 223-231. <http://dx.doi.org/10.1080/19475683.2015.1007894>
- [19]. USGS, (2015). Landsat 8 (L8) Data Users Handbook, LSDS-1574 Version 1.0, Department of the Interior, U.S. Geological Survey, pp. 3.
- [20]. USGS, (2019). Landsat 8 (L8) Data Users Handbook, LSDS-1574 Version 5.0, Department of the Interior, U.S. Geological Survey, pp. 3.
- [21]. John C. (2012). PANCROMA™ Satellite Image Processing Making Satellite Better™, Instruction Manual Version 101, pp. 1-399, www.PANCROMA.com.
- [22]. Landsat Technical Guide, (2004). Global Land Cover Facility, University of Maryland Institute for Advanced Computer Studies, Department of Geography, http://ftpwww.gsfc.nasa.gov/IAS/handbook/handbook_toc.html, pp. 1-2.
- [23]. Acharya, T. D., Subedi, A., Huang, H. and Lee, D. H. (2019). Application of Water Indices in Surface Water Change Detection using Landsat Imagery in Nepal, Sensors and Materials, Vol. 31, No. 5, pp. 1429-1447. <https://doi.org/10.18494/SAM.2019.2264>
- [24]. Tuan, A. V., Hang, L. T. T. and Quang, N. H. (2019). Monitoring Urban Surface Water Bodies Changes using MVDWI Estimated from Pan-sharpened Optical Satellite Images, Fig Working Week, Geospatial Information for a Smarter Life and Environmental Resilience Hanoi, Vietnam, April 22-26, 2019, pp. 1-15.
- [25]. Abazaj, F. (2020). Sentinel-2 Imagery for Mapping and Monitoring Flooding in Buna River Area, J. Int. Environment Application & Science, Vol. 15, No. 2, pp. 45-53.
- [26]. Ganaie, H. A., Hashia, H. and Kalota, D. (2013). Delineation of Flood Prone Area using Normalized Difference Water Index (NDWI) and Transect Method: A Case Study of Kashmir Valley, International Journal of Remote Sensing Applications, Vol. 3, No. 2, pp. 53-58.
- [27]. Klemenjak, S., Waske, B., Valero, S. and Chanussot, J. (2012). Unsupervised River Detection in Rapideye Data, IGARSS, pp.

- 6860-6863. 978-1-4673-1159-5/12/\$31.00
©2012 IEEE
- [28]. Ji, L., Zhang, L. and Wylie, B. (2009). Analysis of Dynamic Thresholds for the Normalized Difference Water Index, *Photogrammetric Engineering & Remote Sensing*, Vol. 75, No. 11, pp. 1307-1317.
- [29]. Gu, Y., Brown, J. F., Verdin, J. P. and Wardlow, B. (2007). A Five-year Analysis of MODIS NDVI and NDWI for Grassland Drought Assessment over the Central Great Plains of the United States, *Geophysical Research Letters*, Vol. 34, pp. 1-6. doi:10.1029/2006GL029127
- [30]. Serrano, J., Shahidian, S. and Silva, J. M. (2019). Evaluation of Normalized Difference Water Index a Tool for Monitoring Pasture Seasonal and Inter-Annual Variability in Mediterranean Agro-Silvo-Pastoral System, *Water*, Vol. 11, No. 62, pp. 1-20. doi:10.3390/w11010062
- [31]. Himmelstoss, E. A. (2009). DSAS 4.0 Installation Instruction and User Guide in Thieler, E. R., Himmelstoss, E. A., Zichichi, J. L. and Ergul, A. 2009 Digital Shoreline Analysis System (DSAS) Version 4.0 – An ArcGIS Extension for Calculating Shoreline Change: U.S Geological Survey Open-File Report 2008-1278.